

# Radiation-damage-free ghost diffraction with atomic resolution

Zheng Li,<sup>1,2,3,\*</sup> Nikita Medvedev,<sup>1,2</sup> Henry N. Chapman,<sup>1,2,4</sup> and Yanhua Shih<sup>5,†</sup>

<sup>1</sup>*Center for Free-Electron Laser Science, DESY, Notkestraße 85, D-22607 Hamburg, Germany*

<sup>2</sup>*Hamburg Centre for Ultrafast Imaging, Luruper Chaussee 149, D-22761 Hamburg, Germany*

<sup>3</sup>*SLAC National Accelerator Laboratory, Menlo Park, California 94025, USA*

<sup>4</sup>*Department of Physics, University of Hamburg, Jungiusstraße 9, D-20355 Hamburg, Germany*

<sup>5</sup>*Department of Physics, University of Maryland, Baltimore County, Baltimore, Maryland 21250, USA*

The X-ray free electron lasers (XFEL) enable diffractive structural determination of protein nanocrystals or single molecules that are too radiation-sensitive for conventional X-ray analysis. However the electronic form factor may be modified during the ultrashort X-ray pulse due to photoionization and electron cascade caused by the intense X-ray pulse. For general X-ray imaging techniques, the minimization of the effects of radiation damage is of the major concern to ensure faithful reconstruction of the structure. Here we show that radiation damage free diffraction can be achieved with atomic spatial resolution, by using X-ray parametric down-conversion (XPDC), and two-color two-photon ghost diffraction. We illustrate that formation of the diffractive patterns satisfies a condition analogous to the Bragg equation, with a resolution that can be as fine as the lattice lengthscale of several Å. Because the samples are illuminated by optical photons of low energy from the entangled pair of optical and X-ray two-photon, they can be free of radiation damage.

The advent of femtosecond X-ray free electron lasers (XFEL) has enabled diffractive structural determination of protein crystals or single molecules that are too radiation-sensitive for conventional X-ray analysis [1–3]. Using X-ray pulses of  $\sim 10$  fs, sufficient diffraction signals could be collected before significant changes occur to the sample [1]. However the electronic form factor may be modified due to photoionization and electron cascade caused by the intense X-ray pulse [4], because  $h\nu_X \gg h\nu_{\text{binding}}$ , where  $h\nu_X$  is the X-ray photon energy and  $h\nu_{\text{binding}}$  is the electron binding energy,  $h$  is the Planck's constant. For general X-ray imaging techniques, minimizing the effects of radiation damage during the imaging procedure is of major concern to guarantee a faithful reconstruction of the structure. Here we show that a radiation-damage-free diffraction is achievable with an atomic spatial resolution, by using the properties of entanglement of optical and X-ray photons, which can be achieved by the X-ray parametric down-conversion (XPDC)[5–7], and two-color two-photon ghost diffraction [8–11]. A hard X-ray pulse generated by XFEL is used to pump a nonlinear medium, either a nonlinear crystal, multi-layer photonic crystal or electron beam of single electrons. Hard X-ray photons are down-converted to two-photon pairs that consist of X-ray and optical photons of wavelength  $\lambda_X$  and  $\lambda_o$ . The optical photons are sent to illuminate the sample crystals or molecules, and the reflected photons are collected with a bucket detector  $D_A$ . The entangled X-ray photons travel a distance and are captured by a pixel photon counting detector  $D_B$ . Based on the basic principle of the ghost imaging procedure, the output pulses of the bucket detector  $D_A$  and

the pixel detector  $D_B$  are sent to a coincidence circuit with certain time gate for counting the joint-detection of the two-photon pairs.

We show here that the joint measurement of optical and X-ray photons can form diffraction patterns, and illustrate that formation of the diffraction patterns satisfies a condition analogous to the Bragg equation, with a resolution that could be as fine as the lattice length scale of several angstrom. Because the samples are illuminated by the optical photons of low energy, they can be free of radiation damage. The ultrabright property of XFEL should be crucial for realization of the proposed scheme, to ensure sufficient two-photon flux and signal strength. Since the diffraction pattern formation is based on photon counting, the requirement for signal intensity is benign. We also show that the analogous Bragg condition can be satisfied with feasible experimental parameters.

An optical pulse from XPDC is directed to illuminate a crystal in the optical arm and while diffraction patterns form by a joint measurement of optical and X-ray photons (Fig. 1). Without loss of generality, we assume that the signal photon has an optical wavelength of  $\lambda_s = \lambda_o$ , and the idler photon has an X-ray wavelength of  $\lambda_i = \lambda_X$ . As the optical photons scatter off lattice planes of inter-plane distance  $d_{hkl} = d$ , the condition for the X-ray photons to form peak in diffraction pattern is

$$2\tilde{m}d \sin \theta = n\lambda_s, \quad (1)$$

for an integer  $n$ .  $\theta$  is the reflection angle of the optical photon and lattice planes of a Miller index  $[hkl]$  (Fig. 2), and  $\vec{p}_B$  is a vector on the plane of the pixel detector. As shown in the Appendix, the magnification factor  $\tilde{m}$  is arising due to photon entanglement, which

\* zheng.li@cfel.de

† shih@umbc.edu

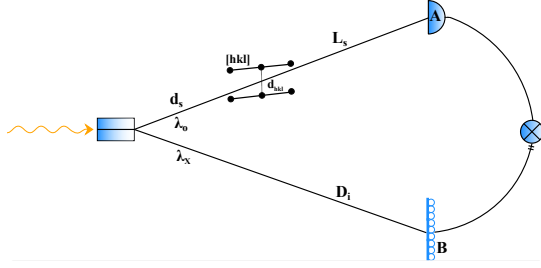


FIG. 1. Proposed layout for two-color two-photon ghost diffraction of entangled X-ray and optical photon pair. The optical photons scatter off lattice planes with Miller index  $[hkl]$  and inter-plane distance  $d_{hkl}$ .

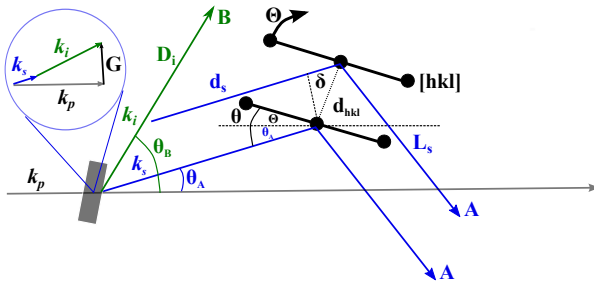


FIG. 2. Sketch of the proposed experiment. The sample is rotated by  $\Theta$ , and its lattice plane forms an angle of  $\theta$  with the incident optical photon in arm A. The relative angle of the X-ray photon (arm B) with the pump photon is determined from the phase matching diagram,  $\vec{k}_s + \vec{k}_i = \vec{k}_p + \vec{G}$ , where  $\vec{G}$  is a reciprocal lattice vector orthogonal to certain atomic planes of a nonlinear crystal,  $\vec{k}_s$ ,  $\vec{k}_i$  and  $\vec{k}_p$  are the wave vectors of the signal, idler and pump fields. And  $z_s = d_s + L_s$ ,  $z_i = D_i$  are the optical path lengths of the signal and idler photons.

can be found as

$$\tilde{m} = 1 - \frac{|\vec{\rho}_B - \vec{d}|^2}{(\alpha + 1) \left( \frac{\lambda_i}{\lambda_s} \right)^2 D_i^2}, \quad (2)$$

where  $\alpha$  is defined as  $\frac{d_s}{D_i} = \alpha \frac{\lambda_i}{\lambda_s}$ .  $\tilde{m}$  guarantees that the Bragg condition (Eq. 1) can be satisfied in the case  $d \ll \lambda_s$ .

The two-photon coincidence counting rate of the bucket detector A and the pixel detector B can be written as [7, 9, 11],

$$R_c(\vec{\rho}_B) = \frac{1}{T} \int dt_A dt_B S(t_B, t_A) \sigma_B \times \text{tr}_{\vec{\rho}_A} \left[ \hat{E}_A^{(-)} \hat{E}_B^{(-)} \hat{E}_B^{(+)} \hat{E}_A^{(+)} \hat{\rho} \right], \quad (3)$$

where  $S(t_B, t_A)$  is the coincidence time function that vanishes unless  $0 \leq t_B - t_A \leq T$ , and describes the finite time gate of a joint-detection of two-photon pair [9].  $\vec{\rho}_A$  is on the plane of bucket detector A with area  $\sigma_A$ ,  $\sigma_B$  is the area of the pixel detector B.  $\rho$  is the density

matrix of the two-photon state on the output plane of the nonlinear crystal.  $E_j^{(+)}$ ,  $j = A, B$  is the positive frequency part of the photon field, and  $E_j^{(-)} = (E_j^{(+)})^\dagger$ .  $\text{tr}_{\vec{\rho}_A}[\dots]$  denotes the trace and coherent summation over  $\vec{\rho}_A$ .  $R_c T$  gives the pixelwise number of counted photons in one joint measurement. The photon fields at the plane of the bucket detector A and the pixel detector B,  $\hat{E}_A^{(+)}$  and  $\hat{E}_B^{(+)}$ , can be calculated as

$$\begin{aligned} \hat{E}_A^{(+)} &= \sum_{\vec{k}_s} g(\vec{k}_s, \omega_s, \vec{\rho}_A, z_s) \hat{a}_s(\vec{k}_s) e^{-i\omega_s t_A} \\ \hat{E}_B^{(+)} &= \sum_{\vec{k}_i} g(\vec{k}_i, \omega_i, \vec{\rho}_B, z_i) \hat{a}_i(\vec{k}_i) e^{-i\omega_i t_B}, \end{aligned} \quad (4)$$

where  $z_s = d_s + L_s$  and  $z_i = D_i$  are the full optical path lengths for the signal and idler photon.  $\vec{k}$  is the transverse momentum of photon field with  $\vec{k} = \sqrt{k^2 - \kappa^2} \hat{e}_z + \vec{\kappa}$ .  $\hat{a}_p^\dagger(\vec{k})$  and  $\hat{a}_p(\vec{k})$  are operators of signal and idler photon field in a specific mode at the output plane of the nonlinear crystal, with the commutator relation,

$$[\hat{a}_p(\vec{k}), \hat{a}_q^\dagger(\vec{k}')] = \delta_{p,q} \delta_{\omega, \omega'} \delta_{\vec{k}, \vec{k}}. \quad (5)$$

$g(\vec{k}, \omega, \vec{\rho}, z)$  is the Green's function for a specific mode of photon field. Assume two atoms in two lattice planes of Miller index  $[hkl]$  with distance  $d = d_{hkl}$  are in a plane  $a$ ,  $\vec{\rho}_a$  is a vector in this plane, and the photon-atom scattering amplitude is  $t(\vec{\rho}_a)$ , the photon fields  $\hat{E}_A^{(+)}$  and  $\hat{E}_B^{(+)}$  at the planes of detectors can be then written as,

$$\begin{aligned} \hat{E}_A^{(+)} &= \sum_{\vec{k}_s} \int d^2 \vec{\rho}_{s'} \int d^2 \vec{\rho}_a \frac{-ik_s}{2\pi d_s} e^{ik_s d_s} e^{i\vec{\kappa}_s \cdot \vec{\rho}_{s'}} e^{i \frac{k_s}{2d_s} |\vec{\rho}_a - \vec{\rho}_{s'}|^2} \\ &\quad \times t(\vec{\rho}_a) \frac{-ik_s}{2\pi L_s} e^{ik_s L_s} e^{i \frac{k_s}{2L_s} |\vec{\rho}_A - \vec{\rho}_a|^2} e^{-i\omega_s t_A} \hat{a}_s(\vec{k}_s) \\ \hat{E}_B^{(+)} &= \sum_{\vec{k}_i} \int d^2 \vec{\rho}_s \frac{-ik_i}{2\pi D_i} e^{ik_i D_i} e^{i\vec{\kappa}_i \cdot \vec{\rho}_s} e^{i \frac{k_i}{2D_i} |\vec{\rho}_s - \vec{\rho}_B|^2} e^{-i\omega_i t_B} \hat{a}_i(\vec{k}_i). \end{aligned} \quad (6)$$

Using a first-order perturbation theory, the two-photon amplitude from an XPDC process is shown to be [?] ]

$$\begin{aligned} \langle 0 | \hat{a}_s(\vec{k}_s) \hat{a}_i(\vec{k}_i) | \Psi \rangle &= -i(2\pi)^3 \gamma \delta(v_s + v_i) \delta(\vec{k}_s + \vec{k}_i) \\ &\quad \times \text{sinc}(v_s D_{si} \frac{L}{2}), \end{aligned} \quad (7)$$

where  $|\Psi\rangle$  is the two-photon state vector,  $\gamma = \frac{\chi^{(2)} E_p L}{2U_s U_i} \sqrt{\frac{\Omega_s \Omega_i T_s T_i c^2}{n_s n_i}}$ ,  $\chi^{(2)}$  is the second-order susceptibility of the nonlinear crystal,  $U_j$  is the group velocity of the signal and idler photon inside the nonlinear crystal of length  $L$ ,  $T_j$  are their transmission coefficients, and  $E_p$  is the strength of the pump field.  $\Omega_s$  and  $\Omega_i$  are the frequencies of signal and idler photons that satisfy

the phase matching condition,  $\omega_p n_p(\omega_p) - \Omega_s n_s(\Omega_s) - \Omega_i n_i(\Omega_i) = 0$ . Provided that the Bragg equation (Eq. 1) and phase matching condition are satisfied, diffraction patterns can be formed on the X-ray photon arm from coincidence photon count in a joint measurement of bucket detector A and pixel detector B, such that the reflection angle  $\theta$  is measured with the detector  $D_A$ , and the corresponding intensity is measured with the detector  $D_B$  from coincidence counts on pixels of given radius  $|\vec{\rho}_B|$ . For the schematic configuration in Fig. 1, the Bragg peaks is manifested as modulation of the coincident counting rate at  $\vec{\rho}_B$  in the plane of pixel detector with a background [12]

$$R_c(\vec{\rho}_B) = \frac{1}{T} \int dt_A dt_B S(t_B, t_A) \sigma_B \left( \frac{\gamma \psi_0}{\pi \lambda_s R_s} \right)^2 \times \left| \int dV_s e^{iV_s \tau_{BA}} \text{sinc}(V_s D_{si} \frac{L}{2}) \right|^2 \times \cos^2 \left[ \frac{2\pi}{\lambda_s R_s} \vec{d} \cdot (\vec{\rho}_B - \frac{\vec{d}}{2}) \right]. \quad (8)$$

$\gamma$  and  $D_{si}$  are parameters of the XPDC process [12],  $D_{si} = \frac{1}{U_s} - \frac{1}{U_i}$ ,  $U_s$  and  $U_i$  are the group velocity of the signal and idler photon inside the nonlinear medium of length  $L$ .  $\tau_{BA} = \tau_B - \tau_A$ , where  $\tau_i = t_i - \frac{r_i}{c}$ ,  $i = A, B$ .  $\psi_0$  is the scattering amplitude of an atom in the lattice with the optical photons, and the effective optical path length from the sample to the pixel detector B,  $R_s = \frac{\lambda_i}{\lambda_s} D_i + d_s$ . We assume the phase matching condition to be  $\Omega_s n_s(\Omega_s) + \Omega_i n_i(\Omega_i) = ck_p$ , ignoring  $\vec{G}$  for simplicity,  $\vec{G}$  can be restored for a given experimental configuration. The frequency of the signal field is  $\omega_s = \Omega_s + \nu_s$ , with  $\nu_s$  characterizing the deviation from the central frequency  $\Omega_s$  of phase matching condition, and  $\nu_s = -\nu_i$ .

For a realistic experiment scenario, we assume an X-ray pulse of 3.1 keV ( $\lambda_i = 4\text{\AA}$ ) and an optical pulse of 3.1 eV ( $\lambda_s = 4000\text{\AA}$ ). Nonlinear x-ray process with energy difference of the two-photon on such scale was experimentally demonstrated [5]. Assume the sample is placed at a distance of 1 cm from the XPDC source, the reflection angle of optical photon is measured on detector  $D_A$ , and the x-ray photon in the two-photon pair is measured by the pixels with radius of 1 m on the pixel detector  $D_B$  placed at a distance of 10 m. In the XFEL nanocrystal diffraction experiment, virtual powder diffraction patterns are formed for various reflection angles, and the single photons from the XPDC process have a certain angular spread [13], it is practically advantageous to determine the actual reflection angle  $\theta$  by a pixel detector  $D_A$ , although in an idealized setup the reflection angle can be uniquely determined by the geometrical configuration of the photon source and a single crystal, for which a bucket detector  $D_A$  is sufficient. The Bragg equation gives the two-color two-photon ghost diffraction pattern shown in Fig. 3. The

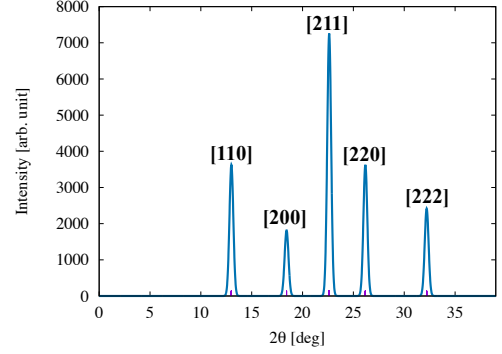


FIG. 3. Simulated two-color two-photon ghost diffraction from a body centered cubic (bcc) crystal with lattice constant  $a = b = c = 4\text{\AA}$ . Optical photons of 3.1 eV are used to illuminate the sample crystal. Miller index are labelled for the Bragg peaks. The broadening of Bragg peaks is determined by Scherrer equation (Eq. 9) for a nanocrystal of 100 nm size.

resolution requirement can be satisfied with the state-of-the-art pixel pnCCD detector that can achieve  $75\mu\text{m}$  pixel pitch [1]. The requirement to the spectral and angular resolution of the diffractometer is determined by  $\frac{\Delta d}{d} + \cot \theta \Delta \theta = \frac{\Delta \lambda_s}{\lambda_s}$ , which is on the same scale as the conventional Laue diffraction. For nanocrystals with size  $L_c$ , the Scherrer equation is found to be [12]

$$B = \frac{2\lambda_s}{L_c \cos \theta \tilde{m}}, \quad (9)$$

which determines the width  $B$  of Bragg peaks. As shown in Fig. 3, the width of Bragg peaks is on the same scale as Laue diffraction and is resolvable by the state-of-the-art diffractometer. The optical photon energy of 3.1 eV may fall below band gap of the crystal, and significant absorption can be avoided. Thus the proposed two-color two-photon ghost diffraction scheme could eventually achieve atomic scale resolution without radiation damage.

The physical mechanism of the two-color two-photon ghost diffraction may be understood from the following considerations. The collective scattering of optical photons with the atoms of a crystal or molecule can be described with van Hove's formalism [16]. The scattering cross section can be written as a product of the cross section of scattering on an individual atom and the dynamic structure factor, which defines the collective response of atoms. The cross section of individual scattering is the Thomson scattering cross section with momentum transfer  $\vec{Q}$ ,  $\frac{d\sigma(\vec{Q})}{d\Omega_{\text{th}}} = \frac{r_e^2}{2} (1 + \cos^2 \theta) |f(\vec{Q})|^2$ , provided the optical photons are unpolarized, and  $r_e$  is the classical electron radius  $r_e \simeq 2.82\text{ fm}$ , and  $f(\vec{Q})$  is the form factor. For the photons as particles, the probability of

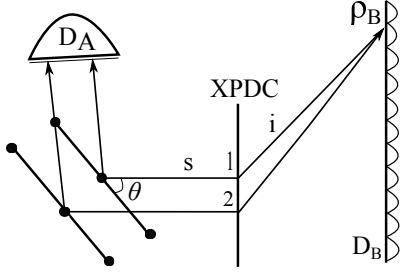


FIG. 4. Unfolded two-photon diagram of the proposed experimental setup.

reflection from atom is on the same orders of magnitude for the optical and x-ray photons. Without considering the molecular form factor of  $f(\vec{Q})$ , we could model the form factor of a crystal as periodic distributions of point scatters as  $f(\vec{Q}) = -r_e \delta(\vec{Q} - 2\pi\vec{G}_{hkl})$ , where  $\vec{G}_{hkl}$  is the reciprocal vector with  $|\vec{G}_{hkl}| = \frac{1}{d_{hkl}}$ . However, for the scattering of optical photon and atoms, the momentum transfer  $\vec{Q} = 2\frac{\omega_s}{c} \sin \theta (-\cos \phi \cos \theta, -\sin \phi \cos \theta, \sin \theta)$ , which is proportional to the incident photon energy, is too small for the optical photon to form interference patterns that  $\vec{Q} \ll \vec{G}_{hkl}$ . Thus Laue diffraction requires X-ray photons of wavelength  $\lambda < 2d$ .

The momentum transfer can be effectively magnified in the two-photon ghost diffraction from  $\vec{Q}$  to  $\tilde{m}\vec{Q}$ . The mechanism of momentum transfer magnification can be understood by a simple quantum model of “unfolded” two-photon ghost diffraction [14] in Fig. 4. In the simplified scenario, the photon fields on detectors  $D_A$  and  $D_B$  can be written as

$$\begin{aligned}\hat{E}_A^{(+)} &= \hat{a}_{1s} e^{ik_s r_{A1}} + \hat{a}_{2s} e^{ik_s r_{A2}} \\ \hat{E}_B^{(+)} &= \hat{a}_{1i} e^{ik_i r_{B1}} + \hat{a}_{2i} e^{ik_i r_{B2}},\end{aligned}\quad (10)$$

where  $\hat{a}_{lp}$ ,  $l = 1, 2$ ,  $p = s, i$  are the annihilation operators of signal and idler photons at position 1, 2 in Fig. 4. The two-photon state  $|\Psi\rangle$  can be expressed as

$$|\Psi\rangle = |0\rangle + \varepsilon [\hat{a}_{1s}^\dagger \hat{a}_{1i}^\dagger e^{i\phi_1} + \hat{a}_{2s}^\dagger \hat{a}_{2i}^\dagger e^{i\phi_2}] |0\rangle, \quad (11)$$

where  $\varepsilon$  is the two-photon amplitude, and we can assume  $\phi_1 = \phi_2$  since the pump beam from XFEL or synchrotron should be transversely coherent at 1 and 2. The two-photon interference is formed due to the uncertainty in the birth place of the two-photon pair (1 or 2 in Fig. 4), and the property of the two-photon product state that allows us to have the uncertainty relation  $\Delta(\vec{k}_s + \vec{k}_i) = 0$  and  $\Delta(\vec{p}_s - \vec{p}_i) = 0$  at the same time [15]. It is straightforward to find the second-order coherence function  $G_{AB} \propto \varepsilon^2 \cos^2 \left[ \frac{\pi}{\lambda_s} (r_{A1} - r_{A2}) + \frac{\pi}{\lambda_i} (r_{B1} - r_{B2}) \right]$ ,

and Bragg peak is formed under condition

$$2d \sin \theta + \frac{\lambda_s}{\lambda_i} (r_{B1} - r_{B2}) = n\lambda_s, \quad (12)$$

In Eq. 12, the Bragg condition can be satisfied despite  $d \ll \lambda_s$ , because the optical path length difference can be compensated by that of the arm of idler photons magnified by a factor  $\frac{\lambda_s}{\lambda_i}$  of  $\sim 10^3$ . As a result, we have a general magnification factor  $\tilde{m}$  as in Eq. 1, and equivalently an effective form factor  $f_{\text{eff}}(\vec{Q}) = -r_e \delta(\tilde{m}\vec{Q} - 2\pi\vec{G}_{hkl})$ , which is able to produce diffraction patterns for reciprocal vectors on the  $1/\text{\AA}$  scale. The collective effects enter the picture via the dynamic structure factor. It is known that the intensity of Bragg peaks is reduced due to the dynamical structural factor  $S(\vec{Q}, \omega_s)$  [16] by a factor of  $\exp \left\{ -\frac{1}{2} \left\langle \left[ \vec{Q} \cdot (\vec{u}_{\vec{R}}(t) - \vec{u}_{\vec{R}}(0)) \right]^2 \right\rangle_T \right\}$ , where  $\vec{u}_{\vec{R}}(t)$  and  $\vec{u}_{\vec{R}}(0)$  are the displacement vectors around  $\vec{0}$  and  $\vec{R}$ , and  $\vec{R}$  is the lattice vector,  $\langle \dots \rangle_T$  denotes the thermal expectation value. However, due to the small momentum transfer  $\vec{Q}$ , the reduction of Bragg peak intensity is substantially weaker than that of Laue diffraction.

In the presented scenario, we assumed that the material under irradiation has a band gap larger than the optical photon energy. Otherwise, because the frequency of the optical photon is much lower than the X-ray photon,  $\omega_o \ll \omega_x$ , the proposed experiment could suffer from strong absorption of photon-bound electron scattering. The photon-bound electron cross section of a photon of frequency  $\omega$  may have a larger cross section than the Thomson cross section  $\sigma_T$ ,  $\sigma(\omega) = \sigma_T \frac{\omega^4}{(\omega_0^2 - \omega^2)^2 + \omega^2 \gamma^2}$ , which in turn means that the frequency of optical photons should be detuned from the spectrum of resonance frequencies in order to avoid strong photoabsorption effect. In this sense, the photons in the extreme ultraviolet (XUV) regime may be the least favorable for the two-color two-photon ghost diffraction. The here proposed ghost diffraction scheme using optical photons to interact with the crystal may potentially suffer from skin effect when the samples are good conductors like copper, which has  $\sim 3$  nm skin depth for optical photons in the visible and ultraviolet regime, and optical photons can only penetrate uppermost lattice planes. Thus the two-color two-photon ghost diffraction scheme should be suitable to diffractive structural determination of insulators, semiconductors and protein crystals, which should have poor conductivity. For good conductors, our method may be limited to the cases of thin and homogeneous samples.

In order to achieve sufficient photon counting rate, it is crucially important to have a two-photon source with high flux using X-ray quantum optical techniques [17]. Because the XPDC and the sum-frequency

generation (SFG) processes [5] are subject to the same nonlinear susceptibility, we can expect the feasibility of two-photon production with similar  $\frac{\lambda_s}{\lambda_i}$  ratio. However the strong absorption of X-ray photons by the diamond crystal may significantly suppress the XPDC efficiency. We may use multilayer photonic crystal to enhance quantum efficiency of XPDC. Alternatively we can attempt to use beam of single electrons as nonlinear medium for XPDC, such as by a three-color Kapitza-Dirac effect [18]. Using a time-dependent perturbation theory to the continuum electron wave function of momentum  $\vec{p}$  [18, 19], we find the probability of effective XPDC of three photon beams of optical and X-ray frequencies,  $\omega_{o1}, \omega_{X2}$  and  $\omega_{X3}$ , which satisfy the phase matching condition  $\vec{k}_{X3} = \vec{k}_{o1} + \vec{k}_{X2}$ , to be  $P(\omega_{o1}, \omega_{X2}, \omega_{X3}) = \left| \frac{P_z E_{o1} E_{X2} E_{X3} (3\omega_{o1} + 3\omega_{X2} + 4\omega_{X3})}{8m_e c^2 (\omega_{o1} + \omega_{X2} + \omega_{X3}) \omega_{o1} \omega_{X2} \omega_{X3}} \right|^2 \delta(E_{fi})$ . In the three-color Kapitza-Dirac process, the electrons are scattered  $|\vec{p}_i\rangle \rightarrow |\vec{p}_f\rangle = |\vec{p}_i \pm (\vec{k}_{o1} + \vec{k}_{X2} + \vec{k}_{X3})\rangle$ , and  $\delta(E_{fi}) = \delta(p_f^2/2 - p_i^2/2)$  ensures the energy conservation of the electrons, and  $p_z$  is the initial longitudinal momentum of the electrons. With an intensity  $I \sim 10^{18} \text{W/cm}^2$ , the XPDC probability could reach  $10^{-5}$ .

In conclusion, we have theoretically described a

mechanism to realize X-ray diffraction with atomic scale resolution by two-color two-photon ghost diffraction. Because the sample is irradiated by photons of optical wavelength, the proposed scheme can be free of radiation damage of X-ray photons. In principle the proposed scheme could also be applied for single molecules, to determine the molecular structure using phase retrieval techniques of coherent diffractive imaging. Moreover, achieving resolution on a much smaller length scale than the wavelength of the illuminating photons using quantum product state of fundamental particle entanglement may shed light on future development of quantum-optics-based imaging techniques.

## ACKNOWLEDGMENTS

We thank the Hamburg Centre for Ultrafast Imaging for financial support. We are grateful to Tao Peng, Jochen Schneider, Nina Rohringer, Ivan Vartanyants, Ralf Röhlsberger, Robin Santra, Oriol Vendrell, Jerome Hastings, Lida Zhang and Xiaolei Zhu for stimulating discussions on various aspects of the study. Z.L. is thankful to the Volkswagen Foundation for a Paul-Ewald postdoctoral fellowship.

- 
- [1] A. Barty et al., *Nature Photonics* **6**, 35 (2012).
  - [2] J. Spence, *Nature Photonics* **2**, 390 (2008).
  - [3] Y. Nishino, Y. Takahashi, N. Imamoto, T. Ishikawa, and K. Maeshima, *Phys. Rev. Lett.* **102**, 018101 (2009).
  - [4] H. Quiney and K. A. Nugent, *Nature Phys.* **7**, 142 (2011).
  - [5] T. E. Glover et al., *Nature* **488**, 603 (2012).
  - [6] K. Tamasaku, K. Sawada, E. Nishibori, and T. Ishikawa, *Nature Phys.* **7**, 705 (2011).
  - [7] S. Schwartz et al., *Phys. Rev. Lett.* **109**, 013602 (2012).
  - [8] T. B. Pittman, Y. H. Shih, D. V. Strekalov, and A. V. Sergienko, *Phys. Rev. A* **52**, R3429 (1995).
  - [9] A. Strekalov, A. V. Sergienko, D. N. Klyshko, and Y. H. Shih, *Phys. Rev. Lett.* **74**, 3600 (1995).
  - [10] G. Scarcelli, V. Berardi, and Y. H. Shih, *Phys. Rev. Lett.* **96**, 063602 (2006).
  - [11] M. H. Rubin and Y. H. Shih, *Phys. Rev. A* **78**, 033836 (2008).
  - [12] M. H. Rubin, *Phys. Rev. A* **54**, 5349 (1996).
  - [13] Appendix .
  - [14] K. Tamasaku and T. Ishikawa, *Phys. Rev. Lett.* **98**, 244801 (2007).
  - [15] L. Van Hove, *Phys. Rev.* **95**, 249 (1954).
  - [16] D. N. Klyshko, *Usp. Fiz. Nauk* **154**, 133 (1988).
  - [17] A. Einstein, B. Podolsky, and N. Rosen, *Phys. Rev.* **47**, 777 (1935).
  - [18] B. W. Adams et al., *J Mod. Opt.* **60**, 2 (2013).
  - [19] H. Batelaan, *Rev. Mod. Phys.* **79**, 929 (2007).
  - [20] O. Smirnova, D. L. Freimund, H. Batelaan, and M. Ivanov, *Phys. Rev. Lett.* **92**, 223601 (2004).



## APPENDIX

### Radiation-damage-free ghost diffraction with atomic resolution

Zheng Li,<sup>1,2,3,\*</sup> Nikita Medvedev,<sup>1,2</sup> Henry N. Chapman,<sup>1,2,4</sup> and Yanhua Shih<sup>5,†</sup>

<sup>1</sup>*Center for Free-Electron Laser Science, DESY, Notkestraße 85, D-22607 Hamburg, Germany*

<sup>2</sup>*Hamburg Centre for Ultrafast Imaging, Luruper Chaussee 149, D-22761 Hamburg, Germany*

<sup>3</sup>*SLAC National Accelerator Laboratory, Menlo Park, California 94025, USA*

<sup>4</sup>*Department of Physics, University of Hamburg, Jungiusstraße 9, D-20355 Hamburg, Germany*

<sup>5</sup>*Department of Physics, University of Maryland,  
Baltimore County, Baltimore, Maryland 21250, USA*

---

\* [zheng.li@cfel.de](mailto:zheng.li@cfel.de)

† [shih@umbc.edu](mailto:shih@umbc.edu)

TABLE I. Symbol table.

Symbol	Explanation
$R_c$	counting rate of joint photon detection
$ \Psi\rangle$	two-photon state
$\hat{\rho}$	density matrix of the two-photon state on the output plane of the nonlinear medium
$\hat{E}_A^{(+)}$	positive frequency part of the quantized photon field on the plane of bucket detector A
$\hat{E}_B^{(+)}$	positive frequency part of the quantized photon field on the plane of pixel detector B
$\hat{E}_A^{(-)}$	negative frequency part of the quantized photon field on the plane of bucket detector A
$\hat{E}_B^{(-)}$	negative frequency part of the quantized photon field on the plane of pixel detector B
$\hat{a}_p^\dagger(\vec{k})$	photon creation operator for specific mode $\vec{k}$ and channel $p$ , $p = s, i$
$\hat{a}_p(\vec{k})$	photon annihilation operator for specific mode $\vec{k}$ and channel $p$ , $p = s, i$
$\vec{k}_s$	wave vector of the signal photon
$\vec{k}_i$	wave vector of the idler photon
$k_s$	$ \vec{k}_s $
$k_i$	$ \vec{k}_i $
$\vec{k}_s$	transverse momentum of the signal photon
$\vec{k}_i$	transverse momentum of the idler photon
$\vec{Q}$	momentum transfer of the photon-atom scattering
$\lambda_s$	wavelength of the signal photon
$\lambda_i$	wavelength of the idler photon
$\vec{\rho}_A$	position vector on the plane of bucket detector A
$\vec{\rho}_B$	position vector on the plane of pixel detector B
$\vec{\rho}_a$	position vector on the crystal plane of specific Miller index
$\vec{\rho}_s$	position vector for the signal photon on the output plane of the nonlinear medium
$\vec{\rho}_{s'}$	position vector for the idler photon on the output plane of the nonlinear medium
$\vec{d}$	distance vector between two atoms in the crystal plane of specific Miller index
$d$	$ \vec{d} $
$d_s$	distance from the output plane of the nonlinear medium to the lattice plane of the crystal
$L_s$	distance from the lattice plane to the bucket detector A
$D_i$	distance from the output plane of the nonlinear medium to the pixel detector B
$R_s$	$d_s + \frac{\lambda_s}{\lambda_s} D_i$
$z_s$	$d_s + L_s$
$z_i$	$D_i$
$\omega_s$	frequency of the signal photon
$\omega_i$	frequency of the idler photon
$\Omega_s$	central frequency of the signal photon subject to phase matching condition
$\Omega_i$	central frequency of the idler photon subject to phase matching condition
$U_{AB}$	joint photon detection amplitude
$V(\vec{\rho}_A, \vec{\rho}_B)$	interference kernel in the joint photon detection amplitude
$G( \vec{\alpha} , \beta)$	$e^{i\frac{\beta}{2} \vec{\alpha} ^2}$
$\delta$	difference of optical path lengths
$\theta$	reflection angle of the optical photon from the crystal
$\psi_0$	photon-atom scattering amplitude
$\tilde{m}$	magnification factor
$\mathcal{L}(\theta)$	line shape of Bragg peak with reflection angle $\theta$
$L_c$	length of a nanocrystal
$\frac{d\sigma}{d\Omega_{th}}$	Thomson scattering cross section

The appendix is divided into three sections. Section I describes explicitly the analogous Bragg equation, Eq. (1) and the joint photon counting rate for diffraction pattern formation, Eq. (2). Section II illustrate a simple kinematic description of Laue diffraction for the completeness of the theory presented in Section I. Section III treats the broadening effect of Bragg peaks.

## I. BRAGG EQUATION FOR TWO-COLOR TWO-PHOTON DIFFRACTION

We assume paraxial approximation for the wave vectors of modes  $|\vec{k}\rangle$  of the photon field,  $\vec{k} = \sqrt{k^2 - \kappa^2} \hat{e}_z + \vec{\kappa}$ , with  $k = \frac{\omega}{c} \gg \kappa$  and  $\vec{\kappa} = (k_x, k_y, 0)$ . The two-photon coincidence counting rate of the bucket detector A and the pixel detector can be written as [1–3],

$$R_c(\vec{\rho}_B) = \frac{1}{T} \int dt_A dt_B S(t_B, t_A) \sigma_B \text{tr}_{\vec{\rho}_A} \left[ \hat{E}_A^{(-)} \hat{E}_B^{(-)} \hat{E}_B^{(+)} \hat{E}_A^{(+)} \hat{\rho} \right], \quad (1)$$

where  $S(t_B, t_A)$  is the coincidence time function that vanishes unless  $0 \leq t_B - t_A \leq T$  and can be approximated as a rectangular function,  $\vec{\rho}_A$  and  $\vec{\rho}_B$  are vectors on the plane of bucket detector A with area  $\sigma_A$  and the plane of pixel detector B with area  $\sigma_B$  respectively.  $\hat{\rho}$  is the density matrix of the two-photon state on the output plane of the nonlinear crystal.  $\hat{E}_j^{(+)}$ ,  $j = A, B$  is the positive frequency part of the photon field, and  $\hat{E}_j^{(-)} = (\hat{E}_j^{(+)})^\dagger$ . And  $\text{tr}_{\vec{\rho}_A}[\cdots]$  denotes the trace and coherent summation over  $\vec{\rho}_A$ . We compute the photon fields at the plane of the bucket detector A and the pixel detector B,  $\hat{E}_A^{(+)}$  and  $\hat{E}_B^{(+)}$  as,

$$\begin{aligned}\hat{E}_A^{(+)}(\vec{\mathbf{k}}_s, \vec{k}_s, \vec{\rho}_A, z_s, \omega_s, t_A) &= \sum_{\vec{k}_s} g(\vec{\mathbf{k}}_s, \omega_s, \vec{\rho}_A, z_s) \hat{a}_s(\vec{k}_s) e^{-i\omega_s t_A} \\ \hat{E}_B^{(+)}(\vec{\mathbf{k}}_i, \vec{k}_i, \vec{\rho}_B, z_i, \omega_i, t_B) &= \sum_{\vec{k}_i} g(\vec{\mathbf{k}}_i, \omega_i, \vec{\rho}_B, z_i) \hat{a}_i(\vec{k}_i) e^{-i\omega_i t_B},\end{aligned}\quad (2)$$

where  $z_s = d_s + L_s$  and  $z_i = D_i$  are the full optical path lengths for the signal and idler photon.  $\hat{a}_p^\dagger(\vec{k})$  and  $\hat{a}_p(\vec{k})$  are operators of signal and idler photon field in a specific mode at the output plane of the nonlinear crystal, with the commutator relation,

$$\left[ \hat{a}_p(\vec{k}), \hat{a}_q^\dagger(\vec{k}') \right] = \delta_{p,q} \delta_{\omega, \omega'} \delta_{\vec{k}, \vec{k}'}. \quad (3)$$

$g(\vec{\kappa}, \omega, \vec{\rho}, z)$  is the Green's function for a specific mode of photon field.

Assume two atoms in two lattice planes of Miller index  $[hkl]$  with distance  $d = d_{hkl}$  are in a plane  $a$ ,  $\vec{\rho}_a$  is a vector in this plane (Fig. S1), and the photon-atom scattering amplitude is  $t(\vec{\rho}_a)$ , we shows that  $\hat{E}_A^{(+)}$  and  $\hat{E}_B^{(+)}$  can



be written as [4],

$$\begin{aligned}\hat{E}_A^{(+)} &\equiv \hat{E}_A^{(+)}(\vec{\kappa}_s, \vec{k}_s, \vec{\rho}_A, z_s, \omega_s, t_A) = \sum_{\vec{k}_s} \int d^2 \vec{\rho}_{s'} \int d^2 \vec{\rho}_a \frac{-ik_s}{2\pi d_s} e^{ik_s d_s} e^{i\vec{\kappa}_s \cdot \vec{\rho}_{s'}} e^{i\frac{k_s}{2d_s} |\vec{\rho}_a - \vec{\rho}_{s'}|^2} t(\vec{\rho}_a) \\ &\quad \times \frac{-ik_s}{2\pi L_s} e^{ik_s L_s} e^{i\frac{k_s}{2L_s} |\vec{\rho}_A - \vec{\rho}_a|^2} e^{-i\omega_s t_A} \hat{a}_s(\vec{k}_s) \\ \hat{E}_B^{(+)} &\equiv \hat{E}_B^{(+)}(\vec{\kappa}_i, \vec{k}_i, \vec{\rho}_B, z_i, \omega_i, t_B) = \sum_{\vec{k}_i} \int d^2 \vec{\rho}_s \frac{-ik_i}{2\pi D_i} e^{ik_i D_i} e^{i\vec{\kappa}_i \cdot \vec{\rho}_s} e^{i\frac{k_i}{2D_i} |\vec{\rho}_s - \vec{\rho}_B|^2} e^{-i\omega_i t_B} \hat{a}_i(\vec{k}_i).\end{aligned}\quad (4)$$

Denote  $G(|\vec{\alpha}|, \beta) = e^{i\frac{\beta}{2}|\vec{\alpha}|^2}$ , its two-dimensional Fourier transformation is

$$\int d^2 \vec{\alpha} G(|\vec{\alpha}|, \beta) e^{i\vec{\gamma} \cdot \vec{\alpha}} = i \frac{2\pi}{\beta} G(|\vec{\gamma}|, -\frac{1}{\beta}). \quad (5)$$

The photon field  $\hat{E}_A^{(+)}$  and  $\hat{E}_B^{(+)}$  can be then written as

$$\begin{aligned}\hat{E}_A^{(+)} &= \sum_{\vec{k}_s} \int d^2 \vec{\rho}_a \frac{1}{i\lambda_s L_s} t(\vec{\rho}_a) G(|\vec{\rho}_a - \vec{\rho}_A|, \frac{k_s}{L_s}) e^{i\vec{\kappa}_s \cdot \vec{\rho}_a} G(|\vec{\kappa}_s|, -\frac{d_s}{k_s}) e^{i(k_s z_s - \omega_s t_A)} \hat{a}_s(\vec{k}_s) \\ \hat{E}_B^{(+)} &= \sum_{\vec{k}_i} G(|\vec{k}_i|, -\frac{D_i}{k_i}) e^{i\vec{\kappa}_i \cdot \vec{\rho}_B} e^{i(k_i z_i - \omega_i t_B)} \hat{a}_i(\vec{k}_i).\end{aligned}\quad (6)$$

With Eq. 6, we can obtain explicitly the second-order coherence function in Eq. 1,

$$\begin{aligned}G_{AB} &= \text{tr}_{\vec{\rho}_A} \left[ \hat{E}_A^{(-)} \hat{E}_B^{(-)} \hat{E}_B^{(+)} \hat{E}_A^{(+)} \hat{\rho} \right] \\ &= \left| \int d^2 \vec{\rho}_A \langle 0 | \hat{E}_B^{(+)} \hat{E}_A^{(+)} | \Psi \rangle \right|^2 \\ &\equiv \left| \int d^2 \vec{\rho}_A U_{AB} \right|^2,\end{aligned}\quad (7)$$

where  $|\Psi\rangle$  is the two-photon state vector, and  $U_{AB}$  is the joint photon detection amplitude. Without loss of generality, we ignore here the reciprocal lattice vector  $\vec{G}$  of the nonlinear crystal, which can be added for a given experimental configuration. Suppose the phase matching condition is satisfied for  $\omega_p n_p(\omega_p) - \Omega_s n_s(\Omega_s) - \Omega_i n_i(\Omega_i) = 0$ , with  $K_j = \frac{\Omega_j}{c}$ , and deviation from the central frequency  $\omega_j = \Omega_j + \nu_j$ ,  $j = s, i$ . Frequency and spatial filtering guarantees  $\nu_j \ll \Omega_j$  and  $\kappa_j \ll K_j$ , thus we have

$$\vec{k}_j = \vec{\kappa}_j + (K_j + \frac{\nu_j}{c} + \frac{\nu_j^2}{2\Omega_j c} - \frac{\kappa_j^2}{2K_j}) \hat{e}_z \simeq \vec{\kappa}_j + (K_j + \frac{\nu_j}{c}) \hat{e}_z. \quad (8)$$

Taken Eqs. 6 and 7, we have

$$\begin{aligned}U_{AB} &= \frac{1}{i\lambda_s L_s} e^{i(K_s z_s + K_i z_i - \Omega_s t_A - \Omega_i t_B)} \left[ \sum_{\vec{k}_s, \vec{k}_i} g'_A(\vec{\rho}_A, \nu_s, \vec{\kappa}_s) g'_B(\vec{\rho}_B, \nu_i, \vec{\kappa}_i) \langle 0 | \hat{a}_s(\vec{k}_s) \hat{a}_i(\vec{k}_i) | \Psi \rangle \right] \\ &\equiv \frac{1}{i\lambda_s L_s} e^{i(K_i z_i - \Omega_s t_A - \Omega_i t_B)} U' .\end{aligned}\quad (9)$$

Using a first-order perturbation theory, the two-photon amplitude from a PDC process is shown to be [2, 5],

$$\langle 0 | \hat{a}_s(\vec{k}_s) \hat{a}_i(\vec{k}_i) | \Psi \rangle = -i(2\pi)^3 \gamma \delta(\nu_s + \nu_i) \delta(\vec{\kappa}_s + \vec{\kappa}_i) \text{sinc}(\nu_s D_{si} \frac{L}{2}), \quad (10)$$

where  $\gamma = \frac{\chi^{(2)} E_p L}{2U_s U_i} \sqrt{\frac{\Omega_s \Omega_i T_s T_i c^2}{n_s n_i}}$ ,  $D_{si} = \frac{1}{U_s} - \frac{1}{U_i}$ ,  $U_s$  and  $U_i$  are the group velocity of the signal and idler photon inside the nonlinear crystal of length  $L$ .  $\chi^{(2)}$  is the second-order susceptibility of the nonlinear crystal,  $U_j$  is the group

velocity of the signal and idler photon inside the nonlinear crystal of length  $L$ ,  $T_j$  are their transmission coefficients, and  $E_p$  is the strength of the pump field. Using the relation

$$\sum_{\vec{k}_s} \rightarrow \frac{V_Q}{(2\pi)^3} \int d\vec{k}_s = \frac{V_Q}{(2\pi)^3} \int d^2\vec{k}_s \int d\omega_s \frac{d\omega_{s,z}}{d\omega_s} = \frac{V_Q}{(2\pi)^3 c} \int d^2\vec{k}_s \int d\nu_s \quad (11)$$

$$\hat{a}_s(\vec{k}_s) \rightarrow \frac{c}{V_Q} \hat{a}_s(\vec{k}_s, \nu_s), \quad (12)$$

where  $V_Q$  is the quantization volume. We can write  $U'$  in Eq. 9 as

$$\begin{aligned} U' &= -i(2\pi)^{-3} \gamma \int d\nu_s e^{i\nu_s \tau_{BA}} \text{sinc}(\nu_s D_{si} \frac{L}{2}) \int d^2\vec{\rho}_a \int d^2\vec{k}_s G(|\vec{k}_s|, -\frac{D_i}{k_i}) e^{-i\vec{k}_s \cdot \vec{\rho}_B} G(|\vec{k}_s|, -\frac{d_s}{k_s}) e^{i\vec{k}_s \cdot \vec{\rho}_a} \\ &\quad \times t(\vec{\rho}_a) G(|\vec{\rho}_a|, \frac{k_s}{L_s}) G(|\vec{\rho}_A|, \frac{k_s}{L_s}) e^{-i\frac{k_s}{L_s} \vec{\rho}_a \cdot \vec{\rho}_A} e^{iK_s z_s} \\ &\equiv -i\gamma \int d\nu_s e^{i\nu_s \tau_{BA}} \text{sinc}(\nu_s D_{si} \frac{L}{2}) \int d^2\vec{\rho}_a I_{\vec{k}_s} t(\vec{\rho}_a) G(|\vec{\rho}_a|, \frac{k_s}{L_s}) G(|\vec{\rho}_A|, \frac{k_s}{L_s}) e^{-i\frac{k_s}{L_s} \vec{\rho}_a \cdot \vec{\rho}_A} e^{iK_s z_s}, \end{aligned} \quad (13)$$

where  $\tau_{BA} = \tau_B - \tau_A$ ,  $\tau_i = t_i - \frac{r_i}{c}$ ,  $i = A, B$ , and  $r_i$  are the full lengths of the optical paths. Define the effective sample-to-pixel detector path length  $R_s = d_s + \frac{\lambda_i}{\lambda_s} D_i$ , the integral  $I_{\vec{k}_s}$  over transverse momentum  $\vec{k}_s$  in Eq. 13 can be rewritten as

$$\begin{aligned} I_{\vec{k}_s} &= \frac{1}{(2\pi)^3} \int d^2\vec{k}_s G(|\vec{k}_s|, -(\frac{D_i}{k_i} + \frac{d_s}{k_s})) e^{i\vec{k}_s \cdot (\vec{\rho}_a - \vec{\rho}_B)} \\ &= \frac{1}{(2\pi)^3} (-i) \frac{2\pi}{\frac{D_i}{k_i} + \frac{d_s}{k_s}} G(|\vec{\rho}_a - \vec{\rho}_B|, \frac{1}{\frac{D_i}{k_i} + \frac{d_s}{k_s}}) \\ &= \frac{1}{2\pi} \frac{1}{i\lambda_s R_s} G(|\vec{\rho}_a - \vec{\rho}_B|, \frac{K_s}{R_s}), \end{aligned} \quad (14)$$

because  $\frac{D_i}{k_i} + \frac{d_s}{k_s} = \frac{1}{2\pi} (D_i \lambda_i + d_s \lambda_s) = \frac{\lambda_s}{2\pi} (D_i \frac{\lambda_i}{\lambda_s} + d_s) = \frac{R_s}{K_s}$ . The amplitude for joint photon detection at the bucket detector A and the pixel detector B is then

$$\begin{aligned} U_{AB} &= \langle 0 | \hat{E}_B^{(+)} \hat{E}_A^{(+)} | \Psi \rangle = -\frac{\gamma}{\lambda_s L_s} e^{i(K_i z_i - \Omega_s t_A - \Omega_i t_B)} \int d\nu_s e^{i\nu_s \tau_{BA}} \text{sinc}(\nu_s D_{si} \frac{L}{2}) \\ &\quad \times \left\{ \frac{e^{iK_s z_s}}{2\pi i \lambda_s R_s} G(|\vec{\rho}_A|, \frac{K_s}{L_s}) G(|\vec{\rho}_B|, \frac{K_s}{R_s}) \int d^2\vec{\rho}_a t(\vec{\rho}_a) G(|\vec{\rho}_a|, K_s (\frac{1}{L_s} + \frac{1}{R_s})) e^{-iK_s (\frac{\vec{\rho}_B}{R_s} + \frac{\vec{\rho}_A}{L_s}) \cdot \vec{\rho}_a} \right\} \\ &\equiv -\frac{\gamma}{\lambda_s L_s} e^{i(K_i z_i - \Omega_s t_A - \Omega_i t_B)} \int d\nu_s e^{i\nu_s \tau_{BA}} \text{sinc}(\nu_s D_{si} \frac{L}{2}) V(\vec{\rho}_A, \vec{\rho}_B), \end{aligned} \quad (15)$$

where  $V(\vec{\rho}_A, \vec{\rho}_B)$  is the interference kernel of the joint photon detection amplitude  $U_{AB}$  that characterizes the formation of the two-photon diffraction pattern. We now consider the scattering of the optical photon with the atoms in a lattice by integrating over  $\vec{\rho}_a$ , and the collection of optical photons at the bucket detector A by integrating over  $\vec{\rho}_A$  in the detector plane, because the bucket detector collects photons without distinguishing their actual position. We expect that diffraction patterns can be formed on the image plane of the pixel detector B, with intensity  $I(\vec{\rho}_B)$  and joint photon counting rate  $R_c(\vec{\rho}_B)$  at  $\vec{\rho}_B$

$$I(\vec{\rho}_B) = R_c(\vec{\rho}_B) T \sim \left| \int d^2\vec{\rho}_A V(\vec{\rho}_A, \vec{\rho}_B) \right|^2. \quad (16)$$

To obtain the analogous Bragg equation for two-color two-photon ghost diffraction, we consider two optical paths  $A_1$  and  $A_2$  of the optical photons that scatter with two atoms in two lattice planes with distance  $d \equiv d_{hkl}$  (Fig. S1). For optical path  $A_1$ , we have

$$\begin{aligned} L_s^{(1)} &= L_s \\ R_s^{(1)} &= d_s + \frac{\lambda_i}{\lambda_s} D_i \equiv R_s \\ z_s^{(1)} &= d_s + D_i \equiv z_s, \end{aligned} \quad (17)$$

and for optical path  $A_2$

$$\begin{aligned} L_s^{(2)} &= L_s \\ R_s^{(2)} &= (d_s + 2\delta) + \frac{\lambda_i}{\lambda_s} D_i \equiv R_s + 2\delta \\ z_s^{(2)} &= (d_s + 2\delta) + D_i \equiv z_s + 2\delta, \end{aligned} \quad (18)$$

where  $\delta = d \sin \theta$ . Thus the effective two-photon joint detection amplitude consists of contribution from the two optical paths,  $V(\vec{\rho}_A, \vec{\rho}_B) = V^{(1)}(\vec{\rho}_A, \vec{\rho}_B) + V^{(2)}(\vec{\rho}_A, \vec{\rho}_B)$ , and  $t(\vec{\rho}_a) = t^{(1)}(\vec{\rho}_a) + t^{(2)}(\vec{\rho}_a) = \psi_0[\delta(\vec{\rho}_a) + \delta(\vec{\rho}_a - \vec{d})]$ , where  $\vec{d} = (d, 0)$ . We write  $V^{(1)}(\vec{\rho}_A, \vec{\rho}_B)$  and  $V^{(2)}(\vec{\rho}_A, \vec{\rho}_B)$  explicitly as

$$\begin{aligned} V^{(1)}(\vec{\rho}_A, \vec{\rho}_B) &= \frac{\psi_0 e^{iK_s z_s}}{2\pi i \lambda_s R_s} G(|\vec{\rho}_A|, \frac{K_s}{L_s}) G(|\vec{\rho}_B|, \frac{K_s}{R_s}) \\ V^{(2)}(\vec{\rho}_A, \vec{\rho}_B) &= \frac{\psi_0 e^{iK_s(z_s + 2\delta)}}{2\pi i \lambda_s (R_s + 2\delta)} G(|\vec{\rho}_A|, \frac{K_s}{L_s}) G(|\vec{\rho}_B|, \frac{K_s}{R_s + 2\delta}) \\ &\quad \times \left\{ G\left(|\vec{d}|, K_s\left(\frac{1}{L_s} + \frac{1}{R_s + 2\delta}\right)\right) e^{-iK_s\left(\frac{\vec{\rho}_B}{R_s + 2\delta} + \frac{\vec{\rho}_A}{L_s}\right) \cdot \vec{d}} \right\}. \end{aligned} \quad (19)$$

Define  $W^{(p)}(\vec{\rho}_B) = \int d^2 \vec{\rho}_A V^{(p)}(\vec{\rho}_A, \vec{\rho}_B)$ , we have

$$\begin{aligned} W^{(1)}(\vec{\rho}_B) &= \frac{\psi_0 L_s}{2\pi R_s} e^{iK_s z_s} G(|\vec{\rho}_B|, \frac{K_s}{R_s}) \\ W^{(2)}(\vec{\rho}_B) &= \frac{\psi_0 e^{iK_s(z_s + 2\delta)}}{2\pi i \lambda_s (R_s + 2\delta)} G(|\vec{\rho}_B|, \frac{K_s}{R_s}) e^{-i\frac{K_s \delta}{R_s^2} |\vec{\rho}_B|^2} e^{i\frac{K_s}{2} \left(\frac{1}{L_s} + \frac{1}{R_s}\right) |\vec{d}|^2} e^{-i\frac{K_s \delta}{R_s^2} |\vec{d}|^2} \\ &\quad \times e^{-iK_s \frac{\vec{\rho}_B}{R_s} \cdot \vec{d}} e^{i\frac{2K_s \delta}{R_s^2} \vec{\rho}_B \cdot \vec{d}} \int d^2 \vec{\rho}_A G(|\vec{\rho}_A|, \frac{K_s}{L_s}) e^{-iK_s \frac{\vec{d}}{L_s} \cdot \vec{\rho}_A} \\ &= \frac{\psi_0 L_s}{2\pi R_s} e^{iK_s z_s} G(|\vec{\rho}_B|, \frac{K_s}{R_s}) e^{i\frac{K_s}{2R_s} (|\vec{d}|^2 - 2\vec{\rho}_B \cdot \vec{d})} e^{iK_s [2\delta(1 - \frac{|\vec{\rho}_B - \vec{d}|^2}{2R_s^2})]}. \end{aligned} \quad (20)$$

Take far-field approximation  $\delta \ll R_s$  that is similar as Laue diffraction, we have

$$\begin{aligned} |W(\vec{\rho}_B)|^2 &= \left| \int d^2 \vec{\rho}_A V(\vec{\rho}_A, \vec{\rho}_B) \right|^2 \\ &= \left( \frac{\psi_0 L_s}{2\pi R_s} \right)^2 \left\{ 2 + e^{i\frac{K_s}{2R_s} (|\vec{d}|^2 - 2\vec{\rho}_B \cdot \vec{d})} e^{iK_s [2\delta(1 - \frac{|\vec{\rho}_B - \vec{d}|^2}{2R_s^2})]} + \text{c.c.} \right\}. \end{aligned} \quad (21)$$

Analogous to the procedure in Sec. II, we obtain the Bragg equation for two-color two-photon ghost diffraction from Eq. 21 by requiring the  $\delta$ -dependent phase to vanish, i.e.

$$\begin{aligned} K_s \left[ 2\delta \left( 1 - \frac{|\vec{\rho}_B - \vec{d}|^2}{2R_s^2} \right) \right] &= 2n\pi \\ \Rightarrow 2d \sin \theta \left[ 1 - \frac{|\vec{\rho}_B - \vec{d}|^2}{2 \left( \frac{d_s}{D_i} + \frac{\lambda_i}{\lambda_s} \right)^2 D_i^2} \right] &= n\lambda_s, \end{aligned} \quad (22)$$

with an integer  $n$ . Define the magnification factor  $\tilde{m}$  as

$$\tilde{m} \equiv \tilde{m}(\vec{\rho}_B, \vec{d}, d_s, D_i, \lambda_i, \lambda_s) = 1 - \frac{|\vec{\rho}_B - \vec{d}|^2}{2 \left( \frac{d_s}{D_i} + \frac{\lambda_i}{\lambda_s} \right)^2 D_i^2}, \quad (23)$$

the Bragg equation can be then written as

$$2\tilde{m}d \sin \theta = n\lambda_s. \quad (24)$$

Provided the Bragg condition is satisfied, and define  $\vec{\rho}_B = (x, 0)$  and  $\vec{d} = (d, 0)$  for simplicity, we can find

$$\begin{aligned} |W(\vec{\rho}_B)|^2 &= \left| \int d^2\vec{\rho}_A V(\vec{\rho}_A, \vec{\rho}_B) \right|^2 \\ &= \left( \frac{\psi_0 L_s}{\pi R_s} \right)^2 \cos^2 \left[ \frac{2\pi}{\lambda_s R_s} d \left( x - \frac{d}{2} \right) \right] \end{aligned} \quad (25)$$

which forms a broad and flat background. Using Eqs. 1, 7, 15 and 25, we arrive at the final equation for the counting rate of joint photon detection

$$\begin{aligned} R_c(\vec{\rho}_B) &= \frac{1}{T} \int dt_A dt_B S(t_B, t_A) \frac{\sigma_B \gamma^2}{\lambda_s^2 L_s^2} \left| \int d\mathbf{v}_s e^{i\mathbf{v}_s \tau_{BA}} \text{sinc}(\mathbf{v}_s D_{si} \frac{L}{2}) \right|^2 \left| \int d^2\vec{\rho}_A V(\vec{\rho}_A, \vec{\rho}_B) \right|^2 \\ &= \frac{1}{T} \int dt_A dt_B S(t_B, t_A) \sigma_B \left( \frac{\gamma \psi_0}{\pi \lambda_s R_s} \right)^2 \left| \int d\mathbf{v}_s e^{i\mathbf{v}_s \tau_{BA}} \text{sinc}(\mathbf{v}_s D_{si} \frac{L}{2}) \right|^2 \cos^2 \left[ \frac{2\pi}{\lambda_s R_s} d \left( x - \frac{d}{2} \right) \right]. \end{aligned} \quad (26)$$

Eq. 26 can be simplified using the relation

$$\begin{aligned} &\int_{-\infty}^{\infty} d\mathbf{v}_s e^{i\mathbf{v}_s \tau_{BA}} \text{sinc}(\mathbf{v}_s D_{si} \frac{L}{2}) \\ &= \frac{2\pi}{D_{si} L} \text{rect}\left(\frac{2\tau_{AB}}{D_{si} L}\right) \\ &= \begin{cases} \frac{2\pi}{D_{si} L}, & -\frac{D_{si} L}{2} \leq \tau_{AB} \leq \frac{D_{si} L}{2} \\ 0, & |\tau_{AB}| > \frac{D_{si} L}{2} \end{cases}, \end{aligned} \quad (27)$$

and the counting rate of joint-detection can be written as

$$R_c(\vec{\rho}_B) = \frac{1}{T} \int dt_A dt_B S(t_B, t_A) \sigma_B \left( \frac{2\gamma \psi_0}{D_{si} L \lambda_s R_s} \right)^2 \text{rect}\left(\frac{2\tau_{AB}}{D_{si} L}\right) \cos^2 \left[ \frac{2\pi}{\lambda_s R_s} d \left( x - \frac{d}{2} \right) \right]. \quad (28)$$

## II. KINEMATIC DESCRIPTION OF LAUE DIFFRACTION

In Section I, the Bragg condition for the two-color two-photon ghost diffraction is obtained from a kinematic scenario. Here we show the conventional Bragg equation can be obtained from similar procedure for the Laue diffraction with monochromatic X-ray beam.

According to Fourier optics, a light wave that passes the plane  $z = 0$ , and arrives at the plane  $z = \Delta$  can be described by the Huygens principle as

$$\begin{aligned} E(x, y, \Delta) &= \int dk_x dk_y e^{i(k_x x + k_y y)} e^{ik_z \Delta} \mathcal{F}[E(x, y, 0)] \\ &= \int dk_x dk_y e^{i(k_x x + k_y y)} e^{i\Delta \sqrt{k^2 - k_x^2 - k_y^2}} \check{E}(k_x, k_y, 0) \\ &\simeq \int dk_x dk_y e^{i(k_x x + k_y y)} e^{i\Delta \left( k - \frac{k_x^2 + k_y^2}{2k} \right)} \check{E}(k_x, k_y, 0) \\ &= \mathcal{F}^{-1} \left\{ e^{i\Delta \left( k - \frac{k_x^2 + k_y^2}{2k} \right)} \check{\Psi}(k_x, k_y, 0) \right\} \\ &= E(x, y, 0) \otimes P(x, y, \Delta), \end{aligned} \quad (29)$$

where  $P(x, y, \Delta)$  is

$$\begin{aligned} P(x, y, \Delta) &= \mathcal{F}^{-1} \left\{ e^{i\Delta k} e^{i\Delta \left( \frac{k_x^2 + k_y^2}{2k} \right)} \right\} \\ &= -\frac{ike^{ik\Delta}}{2\pi\Delta} e^{i\frac{k(x^2 + y^2)}{2\Delta}}. \end{aligned} \quad (30)$$

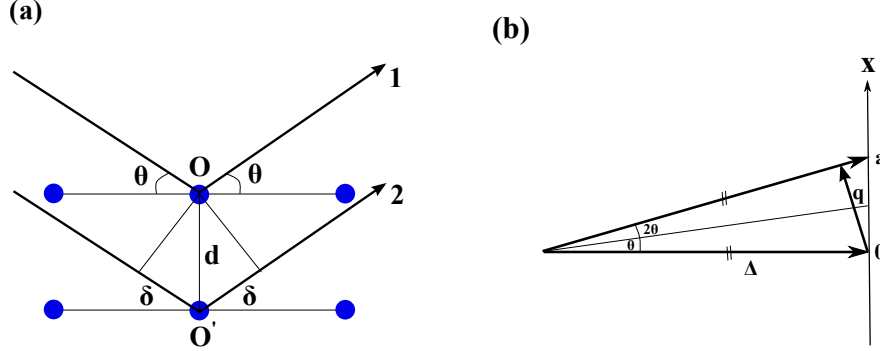


FIG. 2. (a) Optical path diagram for Laue diffraction.  $O$  and  $O'$  are the positions of the atoms in adjacent crystal planes,  $\theta$  is the reflection angle, and  $\delta$  denotes the optical path length difference. (b) Momentum relation of Laue diffraction.  $\Delta$  is the optical path length of the incident and scattered photons along their momentum vectors, and  $\mathbf{q}$  is the momentum transfer.

The physical scenario of Eq. 29 reflects a typical statement of Huygens principle, that (a) the Fourier transformation on the  $z = 0$  plane makes a map to the momentum space  $E(x, y, 0) \rightarrow \check{E}(k_x, k_y, 0)$ , (b) each Fourier mode  $\check{E}(k_x, k_y, 0)$  corresponds to a sub-source that travels as a plane wave  $e^{i(k_x x + k_y y)} e^{ik_z \Delta}$  to the  $z = \Delta$  plane, (c) an inverse Fourier transformation on the  $z = \Delta$  plane gives the image  $E(x, y, \Delta)$ . For Laue diffraction, we follow a standard treatment by considering two optical paths 1 and 2 for photons that scatter off atoms in two lattice planes (Fig. 2(a)). Assume the photon scatters of the two atoms  $O$  and  $O'$  with amplitude  $t^{(1)} = \psi_0 \delta(x - d, y, 0)$  and  $t^{(2)} = \psi_0 \delta(x, y, 0)$ , and denote  $\delta = d \sin \theta$ , we have

$$\begin{aligned}
 E_1(x, y, \Delta) &= \psi_0 \otimes P(x - 0, y - d, \Delta) = -\frac{ik\psi_0 e^{ik\Delta}}{2\pi\Delta} e^{i\frac{k}{2\Delta}[(x-d)^2 + y^2]} \\
 E_2(x, y, \Delta) &= \mathcal{F}^{-1} \left\{ e^{ik_z \delta} \left[ \int dx' dy' e^{-i(k_x x' + k_y y')} \psi_0 \delta(x', y', 0) \right] e^{ik(\Delta + \delta)} e^{-i(\Delta + \delta) \left( \frac{k_x^2 + k_y^2}{2k} \right)} \right\} \\
 &= -\frac{ik\psi_0 e^{ik(\Delta + 2\delta)}}{2\pi(\Delta + 2\delta)} e^{i\frac{k}{2(\Delta + 2\delta)}(x^2 + y^2)}.
 \end{aligned} \tag{31}$$

Thus the intensity of diffraction pattern  $I(x)$  at the detector plane is given by

$$\begin{aligned}
 I(x) &= |E(x, y, \Delta)|^2 = |E_1(x, y, \Delta) + E_2(x, y, \Delta)|^2 \\
 &= \left( \frac{k\psi_0}{2\pi} \right)^2 \left\{ \frac{1}{\Delta^2} + \frac{1}{(\Delta + 2\delta)^2} + \frac{1}{\Delta(\Delta + \delta)} \left[ e^{i\frac{\pi}{\lambda} \left[ \frac{(x-d)^2}{\Delta} - \frac{x^2}{\Delta + 2\delta} \right]} e^{-i\frac{2\pi}{\lambda} 2\delta} + \text{c.c.} \right] \right\} \\
 &= \left( \frac{k\psi_0}{2\pi} \right)^2 I_1.
 \end{aligned} \tag{32}$$

For far-field diffraction  $\Delta \gg 2\delta$ , we have

$$\begin{aligned}
 I_1 &\simeq \frac{1}{\Delta^2} \left\{ 2 + 2 \cos \left[ \frac{\pi}{\lambda \Delta} [(x-d)^2 - x^2] - \frac{2\pi}{\lambda} 2\delta \right] \right\} \\
 &= \frac{2}{\Delta^2} \left\{ 1 + \cos \left[ \frac{\pi}{\lambda \Delta} d(d - 2x) - \frac{2\pi}{\lambda} 2\delta \right] \right\} \\
 &= \left( \frac{2}{\Delta} \right)^2 \cos^2 \left[ \frac{\pi}{\lambda \Delta} d \left( x - \frac{d}{2} \right) - \frac{\pi}{\lambda} 2\delta \right],
 \end{aligned} \tag{33}$$

using the relation  $1 + \cos \alpha = 2 \cos^2 \frac{\alpha}{2}$ .

The Bragg condition is obtained by requiring the  $\delta$ -dependent phase in Eq. 33 to vanish,

$$2\delta = 2d \sin \theta = n\lambda. \quad (34)$$

We obtain the diffraction pattern on the detector with distance  $\Delta$  from the sample,

$$I(x) = \left( \frac{k\psi_0}{\pi\Delta} \right)^2 \cos^2 \left[ \frac{\pi}{\lambda\Delta} d \left( x - \frac{d}{2} \right) \right], \quad (35)$$

with a period  $a = \frac{2\lambda\Delta}{d}$ . Meanwhile, we show that the kinematic description is consistent with the description of Laue diffraction in momentum space. The form factor  $f(\vec{Q})$  is a Fourier transformation of charge distribution. For simplicity, we model the atoms as point charges, thus

$$f(\vec{Q}) = \int d\vec{r} e^{i\vec{Q}\cdot\vec{r}} [\delta(\vec{r}) + \delta(\vec{r} - \vec{d})] = 1 + e^{iQd}, \quad (36)$$

and the intensity of diffraction pattern is

$$I \sim |f(\vec{Q})|^2 = 2(1 + \cos Qd) = 4 \cos^2 \frac{Qd}{2}. \quad (37)$$

From Fig. 2(b), we can find that  $\sin \theta \simeq \frac{x}{2\Delta}$  and

$$Q \equiv |\vec{Q}| = 2|\vec{k}| \sin \theta \simeq 2 \frac{2\pi}{\lambda} \frac{x}{2\Delta} = \frac{2\pi x}{\lambda\Delta} \quad (38)$$

Taken Eqs. 37 and 38, we obtain the intensity of diffraction pattern

$$I(x) \sim |f(\vec{Q})|^2 = 4 \cos^2 \left( \frac{\pi d}{\lambda\Delta} x \right), \quad (39)$$

with a period  $a = \frac{2\lambda\Delta}{d}$ , which is consistent with Eq. 35 from the kinematic description of Laue diffraction.

### III. BROADENING OF BRAGG PEAKS

Analogous to the Scherrer equation, we calculate the width of the Bragg peaks of the two-color two-photon ghost diffraction, which determines the resolution of the proposed scheme. It is especially important for the vital application of XFEL to the diffraction of nanocrystals with a finite size. Suppose nanocrystal of length  $L_c$  that contains  $N$  lattice planes with inter-plane distance  $d$ , such that  $Nd = L_c$ , the accumulated  $\delta$ -dependent phase for the diffraction from  $N$  atoms can be calculated using Eq. 21 as

$$\begin{aligned} \Gamma(\theta) &= \sum_{p=0}^{N-1} e^{ipK_s} \left[ 2\delta \left( 1 - \frac{|\vec{p}_B - \vec{d}|^2}{2R_s^2} \right) \right] \\ &= N e^{i\frac{N-1}{2}K_s(2\tilde{m}d \sin \theta)} \text{sinc} \left[ \frac{N}{2} K_s(2\tilde{m}d \sin \theta) \right]. \end{aligned} \quad (40)$$

Thus the line shape  $\mathcal{L}(\theta)$  of a Bragg peak at a reflection angle  $\theta$  is

$$\mathcal{L}(\theta) = \Gamma^2(\theta) = N^2 \text{sinc}^2 \left[ \frac{N}{2} K_s(2\tilde{m}d \sin \theta) \right]. \quad (41)$$

The width of Bragg peak can be simply found through zeros of the line shape function as

$$\frac{N}{2} K_s(2\tilde{m}d \cos \theta) \Delta\theta = 2\pi. \quad (42)$$

Define the width of the Bragg peak as  $B = 2\Delta\theta$ , we find

$$B = \frac{2\lambda_s}{L_c \cos \theta \tilde{m}}. \quad (43)$$



The factor  $\frac{\lambda_s}{\tilde{m}}$  in the width of Bragg peaks guarantees that the two-color two-photon ghost diffraction should have a similar resolution as the Laue diffraction, i.e. on the atomic scale.

- 
- [1] A. Strekalov, A. V. Sergienko, D. N. Klyshko, and Y. H. Shih, Phys. Rev. Lett. **74**, 3600 (1995).
  - [2] M. H. Rubin and Y. H. Shih, Phys. Rev. A **78**, 033836 (2008).
  - [3] S. Shwartz et al., Phys. Rev. Lett. **109**, 013602 (2012).
  - [4] J. Goodman, *Introduction to Fourier Optics*, Roberts and Company, 2005.
  - [5] M. H. Rubin, Phys. Rev. A **54**, 5349 (1996).